

Morphology on categorical distributions

Silas Nyboe Ørting^[0000-0002-3081-1547], Hans Jacob Teglbyjærg
Stephensen^[0000-0001-8245-0571], and Jon Spørring^[0000-0003-1261-6702]

Department of Computer Science, University of Copenhagen silas@di.ku.dk

Abstract. The categorical distribution is a natural representation of uncertainty in multi-class segmentations. In the two-class case the categorical distribution reduces to the Bernoulli distribution, for which grayscale morphology provides a range of useful operations. In the general case, applying morphological operations on uncertain multi-class segmentations is not straightforward as an image of categorical distributions is not a complete lattice. Although morphology on color images has received wide attention, this is not so for color-coded or categorical images and even less so for images of categorical distributions. In this work, we establish a set of requirements for morphology on categorical distributions by combining classic morphology with a probabilistic view. We then define operators respecting these requirements, introduce protected operations on categorical distributions and illustrate the utility of these operators on two example tasks: modeling annotator bias in brain tumor segmentations and segmenting vesicle instances from the predictions of a multi-class U-Net.

1 Introduction

Uncertainty quantification is an important part of characterizing decisions on image content. Consider the case of multiple annotators each annotating multiple structures in an image. These annotations will be subject to some level of variation. Instead of eliminating this variation using averaging or consensus, it can be used directly as a measure of the annotators uncertainty. A natural representation for this kind of multi-annotator multi-class data is the categorical distribution. Likewise, the categorical distribution arise as a natural representation of predictions from multi-class convolutional neural networks (CNNs).

Regardless of provenance, it will often be relevant with post-processing of these images of categorical distributions. Mathematical morphology is a powerful framework for processing binary and grayscale images but is not directly applicable to categorical images. Binary and grayscale morphology are special cases of morphology on complete lattices [11]. For complete lattices the core operators, dilation and erosion, can be defined using supremum and infimum: for binary morphology using set union and intersection; for grayscale morphology using maximum and minimum under the standard total ordering of the reals. For an in depth treatment of the theoretical foundations of mathematical morphology see [11].

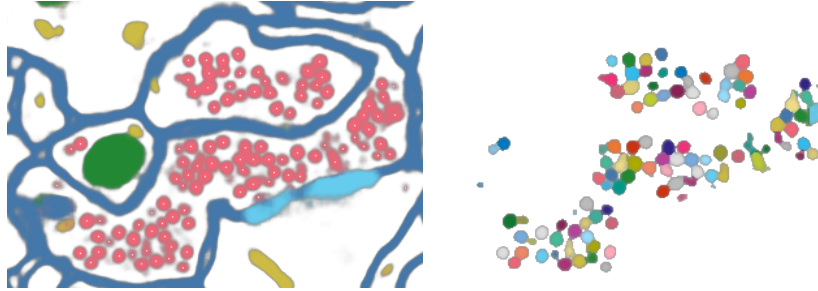


Fig. 1. Seed points and instance segmentation of vesicles using protected erosion.

For multi-valued images, e.g., color and categorical images, the situation is a bit more complicated. Without an ordering of the color- or category-dimension, we cannot define a partial order resulting in a complete lattice. Although morphology on color images has received a lot of attention, see for example the overview in [1], only few works consider morphology on categorical images.

In Hanbury and Serra [5], they consider morphology on the unit circle in the context of angular data. They propose "labeled openings", where the unit circle is partitioned into segments, each segment opened separately and the results combined into a single binary image indicating if a pixel was opened. Although the specific operator could be applied to categorical images, the approach does not lend itself to a general morphology on categorical images.

Busch and Eberle [3] propose a framework where each pixel is assigned a set of categories. This allows a coarse representation of uncertainty, where a pixel can have any combination of categories that are all equally likely. They also propose several variations on the standard operators, including protected operations that do not update a subset of categories. In Ronse and Agnus [9], a framework is proposed where two pseudo-labels, *no label* and *conflicting labels*, are introduced to deal with ambiguity. This results in a binary representation of uncertainty, where uncertainty is either present or not. Although both approaches capture some degree of uncertainty, neither are suitable for varying levels of uncertainty.

Chevallier, Chevallier, and Angulo [4] propose a framework where operations are defined to operate on a single class at a time and propose an extension of this approach to categorical distributions. However, this extension is unsatisfactory for two reasons, openings are not idempotent, meaning that repeated applications do not yield the same result, and it can only deal with boundaries between two objects. A slightly more general version is suggested in [14], though still with single class operations and not extended to categorical distributions.

In this work we establish a set of requirements for morphology on categorical distributions, define operators respecting these requirements, introduce protected operations on categorical distributions, and demonstrate the utility of these operators on two example tasks: modeling annotator bias in brain tumor segmentations, illustrated in Fig. 4, and segmenting vesicle instances from the predictions of a multi-class U-Net, illustrated in Fig. 1

2 Morphology on categorical distributions

The categorical distribution of $n + 1$ categories is completely determined by a point in the n -simplex $\Delta^n = \{a \in \mathbb{R}^{n+1} \mid a_i \geq 0, \sum a_i = 1\}$. Thus, an image A is a function from pixel coordinates to the n -simplex

$$A : \mathbb{Z}^d \mapsto \Delta^n. \quad (1)$$

This leads to the following theorem:

Theorem 1. *Let Δ^n be the n -simplex with $n > 1$ and ' \leq ' be a partial ordering of Δ^n that does not impose an ordering on the $n + 1$ vertices (categories), for example using entropy. The partial order set (poset) (Δ^n, \leq) is not a complete lattice.*

Proof. Assume (Δ^n, \leq) is a complete lattice, then all subsets of Δ^n must have an infimum and a supremum. Let L be any subset of Δ^n , with $\inf L = a$ and $\sup L = b$. Let Q be the set of all permutations of the vertices in a . By definition, \leq must be independent of the order of vertices. Thus $[\forall q \in Q](a \leq q \wedge q \leq a)$. Since a is unique, $Q = \{a\}$. The only element satisfying this is $a = \{1/(n+1)\}^{n+1}$. The same argument holds for b , thus $a = b$. This implies $[\forall l \in L](a \leq l \leq a) \implies L = \{a\}$, which violates the assumption that L is any subset of Δ^n . \square

3 Single category operations

Similarly to [4] we restrict our attention to operations on a single category at a time. The notation to be used in the rest of this article is as follows.

In the following, we restrict our attention to structuring elements B_r which is the closed ball of radius $r > 0$. Let A be an image and x a pixel index, $A(x)$ is then the distribution at x , and A_i the projection of A onto the i 'th category, that is, $A_i(x) = A(x)_i$. We use uppercase letters to refer to a set of categories, e.g., $J = \{j \in [n+1] \mid j \neq i\}$, which is all categories except i . We define $A_J = \sum_{j \in J} A_j$ as the sum over the J categories. We write $T_i(A; B_r)$ for a general morphological operation of category i in image A using structuring element B_r . We use δ for dilation, ϵ for erosion, γ for opening and ϕ for closing. In this article, we will extend existing morphological operations and these will be indicated using the related operation but with a subscript. When we leave out the subscript the operation is standard binary or grayscale morphology, e.g., $\delta(B_1; B_1)$ is the binary dilation of the unit ball with the unit ball, and $\delta(A_i; B_1)$ is the grayscale dilation of A_i with the unit ball.

3.1 Requirements for single category operations

From classic morphology we obtain the following requirements for the four basic operations: dilation, erosion, opening and closing.

Requirement 1. *They are increasing: $A \leq A' \implies T_i A \leq T_i A'$.*

Requirement 2. *Opening is anti-extensive: $\gamma_i A \leq A$.*

Requirement 3. *Closing is extensive: $A \leq \phi_i A$.*

Requirement 4. *Opening and closing are idempotent: $\gamma_i(\gamma_i A) = \gamma_i A$, and $\phi_i(\phi_i A) = \phi_i A$.*

Requirement 5. *Dilation is associative: $\delta_i(\delta_i(A; B_r); B_\rho) = \delta_i(A; \delta(B_r; B_\rho))$.*

Requirement 6. *Erosion satisfies: $\epsilon_i(\epsilon_i(A; B_r); B_\rho) = \epsilon_i(A; \delta(B_r; B_\rho))$.*

For Req. 1–3 to be meaningful we need to impose an order. Since we operate on category i we impose an order based on category i ,

$$A \leq_i A' \iff [\forall x](A_i(x) \leq A'_i(x)). \quad (2)$$

This order yields infimum and supremum for some subsets, but not for all, e.g. there is no infimum or supremum for $\{(0.5, 0.3, 0.2), (0.5, 0.2, 0.3)\}$ under \leq_1 .

For category i , standard grayscale morphology satisfies the six requirements leading us to

Requirement 7. *For category i the operation should be equivalent to operating on the marginal distribution of category i . That is, $(T_i A)_i = T(A_i)$.*

For the remaining categories the order is too weak to uniquely determine operators.

3.2 Requirements from a probabilistic perspective

Since we are working on probability distributions we require that operations yield results that are satisfactory from a probabilistic perspective. Most importantly,

Requirement 8. *For any pixel x , an operation on category i should not change the relative probability of the other categories in $A(x)$.*

Note that Req. 8 implies that dilating category i cannot increase the probability of category $j \neq i$ and erosion cannot decrease the probability of $j \neq i$.

Assume $[\forall x](A_i(x) \in (0, 1))$. We can view $A(x)$ as the expectation of a variable p_x distributed according to a Dirichlet distribution with parameters $\alpha_x = [\alpha_{x,j}]_{j=1\dots n+1} > \mathbf{0}$,

$$A(x) = \mathbb{E}[p_x \sim \text{Dir}(\alpha_x)] = \frac{\alpha_x}{\sum_{k \in [n+1]} \alpha_{x,k}}. \quad (3)$$

From Req. 7, the value $T_i(A)(x)_i = \pi \in (0, 1)$ is known, which together with Req. 8 gives

$$\pi = \frac{\lambda \tilde{\alpha}_{x,i}}{\lambda (\tilde{\alpha}_{x,i} + \sum_{j \neq i} \alpha_{x,j})} \implies \tilde{\alpha}_{x,i} = \frac{\pi}{1 - \pi} \sum_{j \neq i} \alpha_{x,j}. \quad (4)$$

For $k \neq i$ we get

$$T_i(A)(x)_k = \frac{\alpha_{x,k}}{\pi/(1-\pi) \sum_{j \neq i} \alpha_{x,j} + \sum_{j \neq i} \alpha_{x,j}} = (1-\pi) \frac{A(x)_k}{\sum_{j \neq i} A(x)_j}. \quad (5)$$

In general $[\forall x](A(x)_i \in (0, 1))$ is not a reasonable assumption. However, the only problematic case is for erosion when $A(x)_i = 1$, and we will deal with this in Section 3.3.

3.3 Operators

Opening and closing follow from the definition of dilation and erosion. We start with dilation as it is the simpler of the two.

Dilation From Req. 7 and (5) we get

$$\delta_i(A; B_r)(x)_k = \begin{cases} \delta(A_k; B_r)(x), & \text{if } k = i, \\ [1 - \delta(A_i; B_r)(x)] \frac{A_k(x)}{\sum_{j \neq i} A_j(x)}, & \text{if } k \neq i. \end{cases} \quad (6)$$

which is equivalent to the definition from [4].

Erosion Assume $[\forall x](A(x)_i < 1)$. From Req. 7 and (5) we get

$$\epsilon_i(A; B_r)(x)_k = \begin{cases} \epsilon(A_k; B_r)(x) & \text{if } k = i \\ [1 - \epsilon(A_i; B_r)(x)] \frac{A_k(x)}{\sum_{j \neq i} A_j(x)} & \text{if } k \neq i \end{cases} \quad (7)$$

As mentioned above, $[\forall x](A(x)_i < 1)$ is not a reasonable assumption. If we allow $A(x)_i = 1$ we must deal with the case where $A(x)_i = 1$ and $\epsilon(A_i; B_r)(x) < 1$.

$$\epsilon_i(A; B_r)(x)_k = \begin{cases} \epsilon(A_k; B_r)(x) & \text{if } k = i \\ [1 - \epsilon(A_i; B_r)(x)] \frac{A_k(x)}{\sum_{j \neq i} A_j(x)} & \text{if } k \neq i \wedge A(x)_i < 1 \\ [1 - \epsilon(A_i; B_r)(x)] \frac{f(A_k; B_r)(x)}{\sum_{j \neq i} f(A_j; B_r)(x)} & \text{if } k \neq i \wedge A(x)_i = 1 \end{cases} \quad (8)$$

where f is defined such that $\epsilon(A_i; B_r)(x) < 1 \implies [\exists k \neq i] (f(A_k; B_r)(x) > 0)$.

From Req. 6

$$\epsilon_i(\epsilon_i(A, B_r), B_\rho)(x) = \epsilon_i(A, \delta(B_r; B_\rho))(x) = \epsilon_i(A, B_{r+\rho})(x) \quad (9)$$

we get that erosion with a ball of size $r + \rho$ can be decomposed into a series of n erosions using balls of size r_1, r_2, \dots, r_n with $\sum r_i = r + \rho$. Let $r < \rho$. Since f is only used in the case where $A(x)_i = 1$ we must have that

$$\epsilon_i(A; B_r)(x) < 1 \implies \frac{f(A_k; B_\rho)(x)}{\sum_{j \in J} f(A_j; B_\rho)(x)} = \frac{f(A_k; B_r)(x)}{\sum_{j \in J} f(A_j; B_r)(x)} \quad (10)$$

We can then define f as

$$\begin{aligned} f(A_k; B_r)(x) &= \delta(A_k; B_{r^*})(x) \\ r^* &= \arg \min_{r' > 0} r', \text{ s.t. } \epsilon(A_i; B_{r'})(x) < 1 \end{aligned} \quad (11)$$

which states that we use the values from the smallest possible neighborhood.

Theorem 2. *The definition of f in (11) fulfills (9).*

Proof. For brevity we leave out the pixel index x in the following parts. We can ignore f for $k = i$ or $k \neq i$ and $A(x)_i < 1$ and skip that part of the proof.

For $k \neq i$ and $A(x)_i = 1$, $\epsilon(A_i; B_r) = 1$, $\epsilon(A_i; B_{r+\rho}) < 1$ we get after substitution using (8),

$$\epsilon_i(\epsilon_i(A; B_r); B_\rho)(x)_k = [1 - \epsilon(A_i; B_{r+\rho})] \frac{\delta(\epsilon_i(A; B_r)_k; B_{\rho^*})}{\sum_{j \neq i} \delta(\epsilon_i(A; B_r)_j; B_{\rho^*})} \quad (12)$$

$$\rho^* = \arg \min_{\rho' > 0} \rho', \text{ s.t. } \epsilon(e_i(A; B_r)_i; B_{\rho'}) < 1 \quad (13)$$

$$= \arg \min_{\rho' > 0} \rho', \text{ s.t. } \epsilon(A_i; B_{r+\rho'}) < 1 \quad (14)$$

$$= \arg \min_{\rho' > \rho} \rho', \text{ s.t. } \epsilon(A_i; B_{\rho'}) < 1 \quad (15)$$

and

$$\epsilon_i(A; B_{r+\rho})(x)_k = [1 - \epsilon(A_i; B_{r+\rho})] \frac{\delta(A_k; B_{(r+\rho)^*})}{\sum_{j \neq i} \delta(A_j; B_{(r+\rho)^*})} \quad (16)$$

$$(r + \rho)^* = \arg \min_{\varrho > 0} \varrho, \text{ s.t. } \epsilon(A_i; B_\varrho) < 1 \quad (17)$$

$$= \arg \min_{\varrho > r} \varrho, \text{ s.t. } \epsilon(A_i; B_\varrho) < 1 = \rho^* \quad (18)$$

For the second to last line, $\epsilon(A_i; B_r) = 1 \implies \varrho > r$. Thus

$$\epsilon_i(\epsilon_i(A; B_r); B_\rho)(x)_k = \epsilon_i(A; \delta(B_r; B_\rho))(x)_k \quad (19)$$

The case $k \neq i$ and $A(x)_i = 1$, $\epsilon(A_i; B_r) < 1$ can be shown in the same manner. \square

3.4 Opening and closing

We want to show that opening and closing are idempotent,

$$\delta_i(\epsilon_i(\delta_i(A; B_r)(x); B_r)(x); B_r)(x)_k = \delta_i(A; B_r)(x)_k \quad (20)$$

For brevity, we leave out the structuring element B_r , pixel index x and parentheses from operator and function application in the following. For $k = i$ we get,

$$(\delta_i \epsilon_i \delta_i A)_i = \delta \epsilon \delta A_i = \delta A_i = (\delta_i A)_i \quad (21)$$

For $k \neq i$ assume $[\forall x](A_i(x) < 1)$ such that we only deal with the second case in (8). After substitution we get,

$$(\delta_i \epsilon_i \delta_i A)_k = [1 - \delta A_i] \frac{A_k}{\sum_{j \neq i} A_j} = (\delta_i A)_k \quad (22)$$

Now allow $A_i = 1$ in some pixels. The third case in (8) is only relevant in the case where $(\delta_i A)_i = \delta A_i = 1$, thus $1 - \delta A_i = 0$ and

$$(\delta_i \epsilon_i \delta_i A)_k = [1 - \delta A_i] \frac{f(\epsilon_i \delta_i A)_k}{\sum_j f(\epsilon_i \delta_i A)_j} = 0 \quad (23)$$

$$(\delta_i A)_k = [1 - \delta A_i] \frac{A_k}{\sum_j A_j} = 0 \quad (24)$$

So $\delta_i \epsilon_i \delta_i A = \delta_i A$ implying that under the usual definition of opening and closing both are idempotent. This result also shows that the choice of f does not influence idempotence of opening and closing.

3.5 Protected operations

Following [3] we can define operations that protect one or more categories. We call these protected operations. The basic idea for a protected operation is that it should not change the protected categories. Let L be a set of categories, we then write $T_i(A; B_r | L)$ for an operation on i that protects L . If L is empty, or $[\forall x](A_L(x) = 0)$, protected operations reduce to their non-protected counterparts. Otherwise, the requirements

$$\begin{aligned} \delta_i(\delta_i(A; B_r); B_\rho) &= \delta_i(A; \delta(B_r; B_\rho)) \\ \epsilon_i(\epsilon_i(A; B_r); B_\rho) &= \epsilon_i(A; \delta(B_r; B_\rho)) \end{aligned}$$

imply that protected operations should behave as if they were iterated using smaller structuring elements. This has a markedly different impact on dilation and erosion. This difference is illustrated in Fig. 2 and arise because the protected category is restricting the total probability mass available for the other categories, not the relative distribution of this mass. When dilating \heartsuit the protected category \diamond acts as a valve reducing the flow of \heartsuit . After the valve it is not possible to increase the flow to its prior level. When eroding \clubsuit the protected category \diamond acts as if it compresses a container holding \clubsuit and \heartsuit . We can still replace \clubsuit as long as we can reach \heartsuit .

Protected dilation Let J be the set of non-dilated and non-protected categories. Consider protected dilation with the unit ball

$$\delta_i(A; B_1 | L)(x)_k = \begin{cases} A_k & \text{if } k \in L \\ \min(1 - A_L, \delta(A_k; B_1)(x)) & \text{if } k = i \\ [1 - A_L - \delta_i(A; B_1 | L)_i(x)] \frac{A_k(x)}{\sum_{j \in J} A_j(x)} & \text{if otherwise} \end{cases} \quad (25)$$

		$\delta_{\heartsuit}(A; B_1 \diamond)$	$\delta_{\heartsuit}^2(A; B_1 \diamond)$
		$\begin{array}{ccc} x_1 & x_2 & x_3 \\ \hline \clubsuit & 1 & 0 & 0 \\ \diamond & 0 & 0.7 & 0 \\ \heartsuit & 0 & 0.3 & 1 \end{array}$	$\begin{array}{ccc} x_1 & x_2 & x_3 \\ \hline \clubsuit & 0.7 & 0 & 0 \\ \diamond & 0 & 0.7 & 0 \\ \heartsuit & 0.3 & 0.3 & 1 \end{array}$
A		$\epsilon_{\clubsuit}(A; B_1 \diamond)$	$\epsilon_{\clubsuit}^2(A; B_1 \diamond)$
$\begin{array}{ccc} x_1 & x_2 & x_3 \\ \hline \clubsuit & 1 & 0.3 & 0 \\ \diamond & 0 & 0.7 & 0 \\ \heartsuit & 0 & 0 & 1 \end{array}$		$\begin{array}{ccc} x_1 & x_2 & x_3 \\ \hline \clubsuit & 1 & 0 & 0 \\ \diamond & 0 & 0.7 & 0 \\ \heartsuit & 0 & 0.3 & 1 \end{array}$	$\begin{array}{ccc} x_1 & x_2 & x_3 \\ \hline \clubsuit & 0 & 0 & 0 \\ \diamond & 0 & 0.7 & 0 \\ \heartsuit & 1 & 0.3 & 1 \end{array}$

Fig. 2. Difference between protected dilation and protected erosion. For the first erosion we cannot set \clubsuit at x_1 to 0.3 because $\heartsuit = 0$ in all reachable pixels (x_2) and we are not allowed to use \diamond . For the second erosion we can set \clubsuit at x_1 to 0 because $\heartsuit > 0$ in a reachable pixel (x_2)

To obtain the result for a large structuring element we can just iterate using this definition. In practice, we approximate the result using the simplified fast marching method (FMM) from [6] with the update rule defined in [8].

Protected erosion Let $\delta(A; B_r | A_L)$ be the grayscale dilation of A using structuring element B_r on the masked domain $Z = \{x \in \text{dom}(A) \mid A_L(x) < 1\}$. Again consider protected erosion with the unit ball

$$\epsilon_i(A; B_1 | L)(x)_k = \begin{cases} A_k & \text{if } k \in L \\ A_k & \text{if } \sum_{j \in J} \delta(A_j; B_1 | A_L)(x) = 0 \\ \epsilon(A_i; B_1) & \text{if } k = i \\ [1 - A_L - \epsilon(A_i; B_1)] \frac{A_k}{\sum_{j \in J} A_j} & \text{if } \sum_{j \in J} A_j(x) > 0 \\ [1 - A_L - \epsilon(A_i; B_1)] \frac{\delta(A_k; B_1 | A_L)}{\sum_{j \in J} \delta(A_j; B_1 | A_L)} & \text{if otherwise} \end{cases} \quad (26)$$

The second case states that if a pixel and its neighbors are all zero for all categories in J then nothing changes. The third case states that if a pixel is connected to something that is non-zero for any J category, then it can be eroded. The fourth and fifth cases handles normalization.

Similarly to protected dilation we can obtain the general definition through iteration. However, instead of evolving with FMM we can exploit that the protected categories only influence erosion if they completely block all J categories. Let Z be the masked domain as defined above and $d_Z(x, y)$ the distance between pixels x and y in Z . For erosion with a ball of radius r the value of the eroded category in a pixel $x \in Z$ is $\min_{y \in Y} (1 - A_{J \cup L}(y))$, where $Y = \{y \in Z \mid d_Z(x, y) \leq r \wedge A_J(y) > 0\}$. The value of the non-eroded non-protected categories J is then given by rescaling the values of the closest pixels in Y , which is just x if $A_J(x) > 0$.

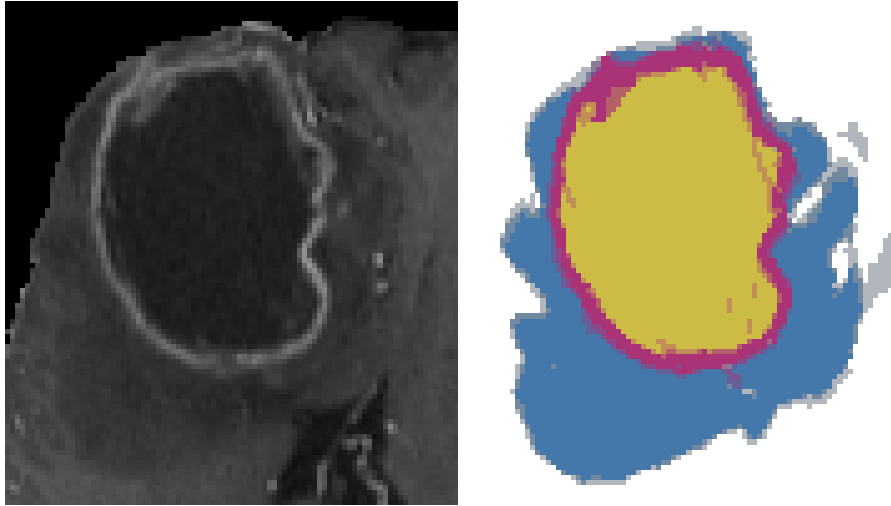


Fig. 3. Inter-rater variation in annotation of brain tumors. White is background, blue edema, yellow inactive core and purple active core. Variation is indicated by color mixing. The primary sources of variation is in the extent of edema and how much of the tumor core is active.

4 Experiments

4.1 Modeling systematic annotator bias in brain tumor segmentations

Expert annotation is the gold standard in most clinical practice as well as for evaluating computer methods. However, annotation tasks are inherently subjective and prone to substantial inter-rater variation [7, 2]. When investigating the influence of this variation on statistics and decisions it can be interesting to consider specific hypotheses regarding the variation. Consider the brain tumor annotation in Fig. 3. The annotation is derived from the QUBIQ¹ challenge brain tumor dataset, where three annotators each annotated whole tumor, tumor core and active tumor. From this we obtain an image with four categories: background, edema, active core, inactive core.

Using protected dilation we can hypothesize how the merged annotation would appear under the assumption that the tumor core should be smaller but more active. Fig. 4 shows the results where we first dilate the active core while protecting edema and background, then dilate edema while protecting background.

¹ <https://qubiq.grand-challenge.org/>

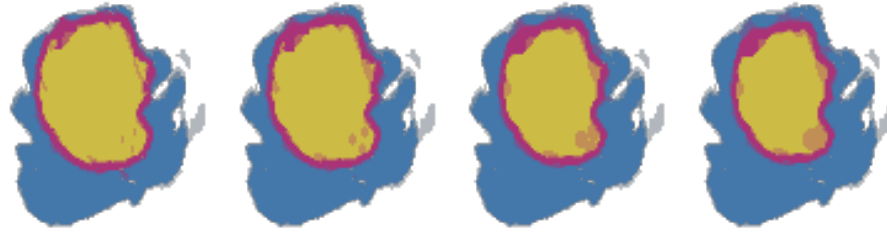


Fig. 4. *What could the annotation look like if the core was oversegmented, but the active part undersegmented?* Left: Annotation. Column 2-4: Dilate active core while protecting edema and background, followed by dilation of edema while protecting background using balls with radius 1, 2, 3.

4.2 Segmenting vesicle instances from U-Net predictions

A common task in microscopy is instance segmentation. Learning instance segmentation directly is certainly possible, see for example [10, 13], it is however quite common to just have class segmentations and a desire for instance segmentations.

Consider the multi-class predictions in Fig. 5 obtained from [12]. Although class separation is quite good, individual vesicles, the red blobs, merge to form large clusters. Using a local maxima method² we can detect instance seed points. Each seed point is then added as a new category to the original predictions and instances are “grown” by eroding the vesicle class, while protecting the other classes. Fig. 1 illustrates the approach. Note that the uncertainty in the original vesicle predictions is preserved and taken into account in intersection points. A similar result could be obtained by assigning each vesicle seed a unique number and applying grayscale dilation. However, this would not restrict instances from jumping across background nor would it be able to handle intersections correctly.

Although the result is not perfect, it is a very easy approach for obtaining high quality instance segmentations from predictions. Further refinement is also possible, for example dilating the large teal vesicle in the right of the image into the dark green vesicle left of it.

5 Discussion & Conclusion

We have established a set of requirements for morphology on categorical distributions, defined operators respecting these requirements, introduced protected operations on categorical distributions and illustrated the utility of these operators on two example tasks: modeling annotator bias in brain tumor segmentations and segmenting vesicle instances from the predictions of a multi-class U-Net.

² https://scikit-image.org/docs/0.17.x/api/skimage.morphology.html#skimage.morphology.local_maxima

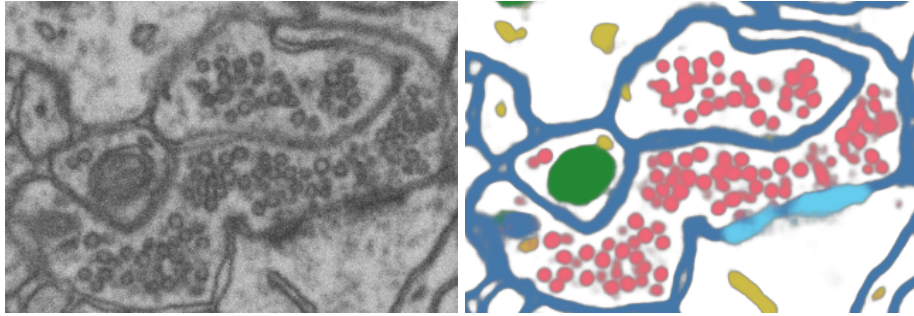


Fig. 5. Electron microscopy image of the hippocampus with predictions of six classes: cytosol (white), membrane (blue), active zone (teal), mitochondria (green), endoplasmic reticulum (yellow), and vesicle (red). We are interested in vesicle instance segmentations.

The definition of dilation is straightforward and no obvious alternatives present themselves. This is not so for erosion. In our definition, erosion corresponds to conditioning on a change in probability of the eroded category. An equally valid approach would be to also condition on where this change came from. Instead of simply rescaling the categories with non-zero mass we would include information from the neighborhood. For example, when eroding i we would fill the difference $A_i(x) - \epsilon(A_i; B_r)(x)$ based on the pixels that contribute to the difference, that is, those with minimum mass for i . This would result in smoother boundaries, which could be a better representation of our uncertainty. A downside is that categories can leak into each other leading to undesirable results. Exploring and comparing alternative definitions of erosion is on the agenda for future work.

The brain tumor and vesicles examples illustrate that protected operations are very useful. In this work we have defined protected dilation and erosion as iterated operations. Since we use FMM to find an approximate solution the results will not exactly match the non-protected counterparts in regions unaffected by the protected categories. At the core of this problem is calculating the exact Euclidean distance on a masked domain. Although likely of small practical importance, as the FMM error is small unless the structuring element is very large, it would be interesting to explore efficient exact Euclidean distance transforms on masked domains.

Due to space limitations we restricted our examples to highlight the protected operations. This is not to imply that non-protected operations are without use. On the contrary, opening is in particular a useful operation, for example for removing speckle noise from multi-class images. More complex operations could also prove useful, such as the morphological gradient, which could be used to investigate spatial relationship between classes by quantifying the change in categories as a function of change in one category.

In conclusion, we have defined morphological operators on categorical distributions and illustrated the utility of these operations for modeling annotator bias and for instance segmentation.

References

1. Aptoula, E., Lefèvre, S.: A comparative study on multivariate mathematical morphology. *Pattern Recognit.* **40**, 2914–2929 (2007)
2. Becker, A.S., Chaitanya, K., Schawkat, K., Muehlematter, U.J., Hötter, A.M., Konukoglu, E., Donati, O.F.: Variability of manual segmentation of the prostate in axial t2-weighted mri: A multi-reader study. *European journal of radiology* **121**, 108716 (2019)
3. Busch, C., Eberle, M.A.: Morphological operations for color-coded images. *Comput. Graph. Forum* **14**, 193–204 (1995)
4. Chevallier, E., Chevallier, A., Angulo, J.: N-ary mathematical morphology. *Mathematical Morphology - Theory and Applications* **1** (2016)
5. Hanbury, A.G., Serra, J.: Morphological operators on the unit circle. *IEEE transactions on image processing* **10**(12), 1842–1850 (2001)
6. Jones, M.W., Baerentzen, J.A., Sramek, M.: 3d distance fields: A survey of techniques and applications. *IEEE Transactions on visualization and Computer Graphics* **12**(4), 581–599 (2006)
7. Joskowicz, L., Cohen, D., Caplan, N., Sosna, J.: Inter-observer variability of manual contour delineation of structures in ct. *European radiology* **29**(3), 1391–1399 (2019)
8. Rickett, J., Fomel, S.: A second-order fast marching eikonal solver. *Stanford Exploration Project Report* **100**, 287–293 (1999)
9. Ronse, C., Agnus, V.: Morphology on label images: Flat-type operators and connections. *Journal of Mathematical Imaging and Vision* **22**, 283–307 (05 2005)
10. Schmidt, U., Weigert, M., Broaddus, C., Myers, G.: Cell detection with star-convex polygons. In: *Medical Image Computing and Computer Assisted Intervention - MICCAI 2018 - 21st International Conference, Granada, Spain, September 16-20, 2018, Proceedings, Part II*. pp. 265–273 (2018)
11. Serra, J.: Morphological filtering: an overview. *Signal processing* **38**(1), 3–11 (1994)
12. Stephensen, H.J., Svane, A.M., Benitez, C., Goldman, S.A., Sporring, J.: Measuring shape relations using r-parallel sets (2020)
13. Stringer, C., Michaelos, M., Pachitariu, M.: Cellpose: a generalist algorithm for cellular segmentation (2020)
14. van de Gronde, J., Roerdink, J.B.: Chapter three - nonscalar mathematical morphology. In: Hawkes, P.W. (ed.) *Advances in Imaging and Electron Physics, Advances in Imaging and Electron Physics*, vol. 204, pp. 111 – 145. Elsevier (2017)